"NDE of Reinforced Concrete Strengthened with Fiber-Reinforced Polymer Composites using Infrared Thermography"

Jeff R. Brown and H.R. Hamilton III
University of Florida – Department of Civil and Coastal Engineering

ABSTRACT

The objective of this research is to investigate various heating and infrared (IR) scanning methods to evaluate the bond between FRP composites and concrete. Experiments were performed on small-scale specimens using IR heating and halogen lamps. A special scanner cart was also designed to facilitate rapid scanning of an FRP surface (approx. 3 ft^2/ min).

Infrared inspections were also performed on four full-scale AASHTO Type II girders that were loaded to failure in the Florida Department of Transportation Structural Testing Facility. Vehicle impact damage was simulated in these girders by cutting several of the girder's prestressing tendons. An FRP strengthening system was then applied to each girder in order to restore its structural capacity. IR thermographic scanning was performed at various stages of loading and after failure in order to monitor the effect of loading on debonded areas.

Keywords: Reinforced Concrete, FRP Strengthening, NDE, Infrared Thermography

INTRODUCTION

The use of fiber-reinforced polymers (FRPs) to strengthen existing civil infrastructure is expanding rapidly. While the short-term performance and strengthening capabilities of FRP composites have been well documented, techniques for evaluating long-term performance (durability) and quality control during installation are still needed. Infrared thermal imaging inspection has been used to evaluate FRP/Concrete bond in both laboratory and field applications in recent years. This technique allows non-contact sensing and a more global range than that of traditional mechanical sounding methods (coin-tap).

An earlier study by Levar and Hamilton (2003) demonstrated that IR thermography is capable of identifying debonded areas between concrete and FRPs. These experiments involved the structural load testing of reinforced concrete beams that had been strengthened in flexure using FRPs. 500 W halogen lamps were used to heat the FRP surface and an IR camera (Raytheon Palm IR250) was used to monitor the surface temperature profile during cooling. Debonded areas appeared as "hot-spots" in the thermal images and patterns of debonding were monitored as each beam was loaded to failure (standard 4-point bending). Important observations from these experiments included the following:

- The total debonded area increased as the load was increased up to failure.
- Certain debonded areas appeared to have different thermal signal strengths.

The above-mentioned infrared thermography experiments were qualitative in nature. The current research objective is to incorporate quantitative IR theral imaging techniques into the inspection process and attempt to draw more detailed conclusions about observed defects. In quantitative thermography, actual surface temperatures are recorded in a thermal image and post-processing of a sequence of images allows for the examination of surface heating and cooling over time. This can reveal important information about defect depth. For multi-layered strengthening systems, it would be useful to differentiate a gap between the concrete and FRP (debond) from a gap between adjacent layers of FRP (delamination). Quantitative techniques can also be used to evaluate the heat-flow characteristics of a known defect over time. Can the presence of moisture or excess resin be differentiated from typical air pockets? Do small problems at the time of installation develop into bigger problems later? The purpose of this paper is to present preliminary results highlighting different heating, IR scanning, and image processing techniques

Most FRP systems applied to civil infrastructure are installed using a “wet-layup” method:

- The concrete surface is first sandblasted and a saturating coat of matrix material is applied. In some instances, an additional tack coat or thickened matrix is also applied.
- The fibers are saturated in a matrix bath and then rolled out onto the concrete. The excess resin is then removed and the system is allowed to cure.
- A gel-coat is applied to the outer surface for additional protection and, if necessary, the system is painted for UV protection.

The degree to which the above steps are performed greatly influences the finished product. The high degree of variability encountered in the field makes the case of FRP bonded to concrete unique. Advanced curing procedures commonly employed in the manufacture of FRP components for the aerospace industry (vacuum assisted, elevated temperature) are not practical in civil engineering applications. As a result, “perfect” installations of FRP strengthening systems are difficult to obtain.

Environmental conditions that make the installation of these systems difficult also raise issues with regards to infrared thermography. These conditions include limited access to the surface being strengthened/inspected and time restraints when vehicle traffic lane closures are required. An important aspect of this research is to identify infrared thermography techniques that can be implemented in the field.

EXPERIMENTAL PROCEDURES

Infrared Thermography Equipment

Thermal images in this study were collected using a FLIR ThermaCAM PM 695 infrared camera. An important feature of this IR camera is the ability to save thermal images digitally. Each pixel in the thermal image (320x240) is stored as a temperature value. This allows for easy post-processing of collected images using FLIR’s ThermaCAM Researcher software. Once a series of thermograms have been selected, areas of interest can be identified and the average temperature in an area can be plotted as a function of time.

Three heat sources were investigated: 500 Watt halogen lamp, IR heating lamps (125 Watt), and a 3200 Joule-second photographer’s flash.

12” x 12” Specimens w/ Fabricated Defects

The first phase of this investigation involved the construction of ten small-scale specimens. Each specimen was constructed using a 12”x12”x2” concrete block. 10”x10” Tyfo SCH-35 carbon-fiber composite patches were applied to each block using the procedure outlined in the introduction, however, no thickened epoxy or tack coat was used. The amount of mixed epoxy required to saturate a single 10”x10” carbon-fiber lamina was approximately 100 ml. The thickness of a single carbon-fiber lamina was 0.035 in. Three specimens served as controls and seven specimens contained various types of fabricated defects. Specific results from two of the experiments will be discussed below.

The general infrared inspection procedure was as follows:

1. A thermal shield was placed between the heat source and the specimen.
2. The pre-warmed 500 Watt halogen lamp was placed 12 inches from the specimen.
3. The shield was removed and thermal images were recorded at 1 frame per 2 seconds as the specimen was heated. The IR camera was approximately 24 inches from the specimen.
4. After a fixed amount of time, t (30 or 60 sec), the halogen lamp was removed and thermal images were recorded as the specimen cooled.

One major problem encountered was the presence of reflected heat energy from the heat source. Figure 1 shows a thermogram for specimen #1 (control) after only two seconds of exposure to the 500-Watt halogen light. The temperature of the specimen prior to removal of the shield was around 32 C, however, the thermal image recorded after two seconds of heating indicates temperatures on the surface of the specimen in excess of 50 C. This is due to infrared radiation generated by the high temperature halogen bulb and then reflected by the specimen.

This problem can be eliminated using an image subtraction feature provided by the Researcher software. As long as neither the thermal imaging camera nor the heat source moves, the amount of reflected IR radiation picked up by the camera remains constant for each pixel in the thermogram sequence. By subtracting the first thermogram image in a sequence from the subsequent images during heating, the reflected radiation is effectively removed. Figure 2 shows results from the same heating sequence with the reflected radiation removed. There are no longer any drastic jumps and all five of the selected areas exhibit the same general heating trend.

Even though the control specimens were intended to be free of defects, infrared inspections did reveal the presence of numerous debonded areas. The pattern of these defects followed the weave of the carbon- fibers. Specifically, areas of the lamina in which the fiber tow ran on top of the fabric's cross-stitch had a tendency to lift off the concrete and form small debonded areas during curing. Defect signal strength results for specimen #1 are presented in Figure 3. Three distinct defects were identified at different positions with respect to the vertical axis and defect signal strength was obtained by subtracting the average temperature of an adjacent defect-free area from the average temperature above the defect. Maximum defect signal strengths of 2.8 °C, 1.4 °C, and 2.4 °C were obtained for defects 1, 2, and 3, respectively.

Since specimen #1 was constructed using a single CFRP lamina, the depth of each debonded area appearing in the thermal image is not in question. It should be noted, however, that the image save rate of 0.5 Hz was inadequate to reveal any information about defect depth. Since the image save rate was not synchronized with the removal of the thermal shield, the first image in the sequence used for subtraction can be as much as two seconds old. Under this worst-case scenario, the first thermal image appearing in the subtracted image sequence can be as much as four seconds old. By this time, the thermal signal has already developed above the defect and the time at which the defect first became visible (a function of its depth beneath the surface) is lost.

Specimen configuration and IR inspection results for specimen #3 are presented in Figures 4 and 5, respectively. All six of the implanted defects in specimen #3 were apparent after 30 seconds of heating with the 500W halogen light. Different defect signal strengths were also obtained due to the different thermal characteristics of the defect material. The most interesting observation relates to the steel defect. Since the steel has a higher thermal conductivity than the surrounding concrete, the surface above the defect becomes cooler than the surrounding areas.

Additional experiments were also performed on the small-scale specimens using 125 Watt IR heat lamps and a 3200 Joule-second photographers flash. The IR heat lamp provided enough heat to reveal the presence of defects, however, the area of heating was limited to a narrow beam. It was necessary to constantly move the lamp across the surface in order to heat the specimen evenly. As a result, it was not possible to collect thermal images of the surface during heating. The 3200 Joule-second photographer's flash worked well for specimens constructed using a single layer of carbon-fiber, however, not enough heat was deposited on the surface to reveal the presence of debonded areas in a four-layer system. Additional work is required to determine the effective limits of this heating technique.

Laboratory IR Inspection of Full-Scale AASHTO Girders Strengthened w/ FRP

The Florida Department of Transportation (FDOT) currently uses FRP strengthening systems to repair bridges that have been damaged by vehicle impact or corrosion. A recent study was conducted by the FDOT in order to pre-qualify FRP system manufacturers for placement on a "Quality Products List". This study involved the structural load testing of full-scale AASHTO Type II prestressed bridge girders that contained simulated vehicle impact damage (achieved by removing concrete and cutting four prestressing strands at midspan). Different manufacturers applied four different FRP strengthening systems (see Table 1) and the girders were then loaded to failure at the FDOT structural research testing facility.

The primary concern for the FDOT was whether or not the applied FRP strengthening system could restore the capacity of the damaged girder to its original strength. Also of interest was determining a suitable NDE method for evaluating the installation of the system as well as a means of performance monitoring throughout its service-life. For this type of flexural strengthening to be effective, the FRP must remain bonded to the surface of the concrete. Any debonds resulting from improper installation or other environmental factors (excessive loading, additional impact, etc…) would reduce the girder's capacity.

The FRP strengthening systems were installed on the bottom face of each girder. Pictures of the specimen and test-setup are provided in Figure 6. The total surface area to which the FRP was applied was 30 ft^2 (1.5 ft x 20 ft) for each beam. The objective of the IR inspection was to first identify any debonded areas immediately after installation and then perform additional inspections as the load on the specimen was increased up to failure. Due to the limited clearance between the floor and the surface being inspected, initial thermal images only captured an area of approximately 9" x 5". The heating methods that were applied to the 12" x 12" specimens proved extremely impractical. It was estimated that a single inspection of the entire system utilizing this method would require over 4 hours (a total of 5 inspections were required for each beam). To facilitate a more rapid inspection, a special scanner cart was designed and fabricated (see Figure 7). The field of view of the IR camera was increased to include the entire 18" width of the FRP by employing first-surface mirrors. Four 125 Watt IR heat lamps were mounted on the cart to heat the surface and thermal images were collected at 2-second intervals as the cart was pushed along on the floor. This method reduced the required inspection time to around 10 minutes. A major limitation to this method is that quantitative thermography techniques become less revealing. Thermal images are not captured while the specimen is being heated and ensuring that the cart is pushed along at a uniform rate to provide uniform heating is difficult.

The FRP strengthening system shown in Figure 8 was constructed using a unique spray-up method in which chopped glass fibers are blown onto the concrete surface along with a vinylester matrix. The thickness of the FRP on the bottom surface varied between 0.3 in. and 0.4 in. Figure 8(a) shows an infrared thermogram of the system at midspan prior to loading. The visible defects in the thermal image are a result of small amounts of fibers falling down before the system fully cured. Some of the defects were formed very near the surface and were easily detectable with the eye. Some of the fainter defects, however, were not readily discernible. Figure 8(b) shows the same area at midspan after the girder failed. The failure mode for this specimen was tensile rupture of the FRP. During rupture, a portion of the FRP expanding outward from the rupture point between 6-8 inches in both directions debonded from the concrete surface. This area was easily detectable via acoustic sounding. The thermal image recorded of this area, however, only reveals a minor variation in surface temperature. The thickness of the FRP system combined with the low thermal conductivity of the glass fibers makes debonded areas difficult to detect. A possible solution would be to introduce more heat to the surface.

Figure 9(a) shows the first layer of a three-layer carbon-fiber system (applied via the wet-layup method described above). The small defects present are similar to those encountered in the 12"x12" control specimens. Unfortunately, after the additional layers of fabric were applied to the surface it became difficult to detect the presence of the debonded areas.

The failure mode for girder #2 was debonding of the applied FRP system. After failure, only a short six-foot portion of the FRP remained bonded at one end. Figure 9(b) shows an IR thermal image taken at the interface between the well-bonded portion and the severely debonded portion after failure. From this image, it is impossible to discern the debonded area. The polyurethane matrix that was used effectively insulated the carbon-fibers from the concrete. Regardless of the amount of heat applied, the temperature on the surface above a debonded area remained the same as above a well-bonded area.

SUMMARY

Results from these experiments indicate that infrared thermal imaging is a potentially powerful tool for evaluating bond between FRP strengthening systems and concrete. By using a thermal imaging system that captures digital images containing pixel-by-pixel temperature data, quantitative analysis of debonded areas is very convenient. Single-layer carbon-fiber systems seem very well suited to the technique, however, the ability the identify defects decreases as the thickness of the FRP increases. Debonded areas beneath fiberglass systems are also difficult to detect. Finally, IR inspections performed on FRP systems containing a polyurethane matrix were not effective.

REFERENCES

1. Levar, J. M. and H. R. T. Hamilton Iii (2003). "Nondestructive evaluation of carbon fiber-reinforced polymer-concrete bond using infrared thermography." ACI Materials Journal **v 100**(n 1): p 63-72.

ACKNOWLEDGEMENTS

The authors would like to thank John Fricot of FLIR Systems for his assistance in obtaining the thermal imaging system used in this study. Additional thanks goes to Marc Ansley and Tom Beitelman of the FDOT Structural Research Center in Tallahassee, Florida. Markus Kutarba, Tony Michael, and Gustavo Alvarez (all graduate students at the University of Florida) also helped with the collection of thermal images. Many thanks to them. Finally, this material is based upon work supported under a National Science Foundation Graduate Research Fellowship.

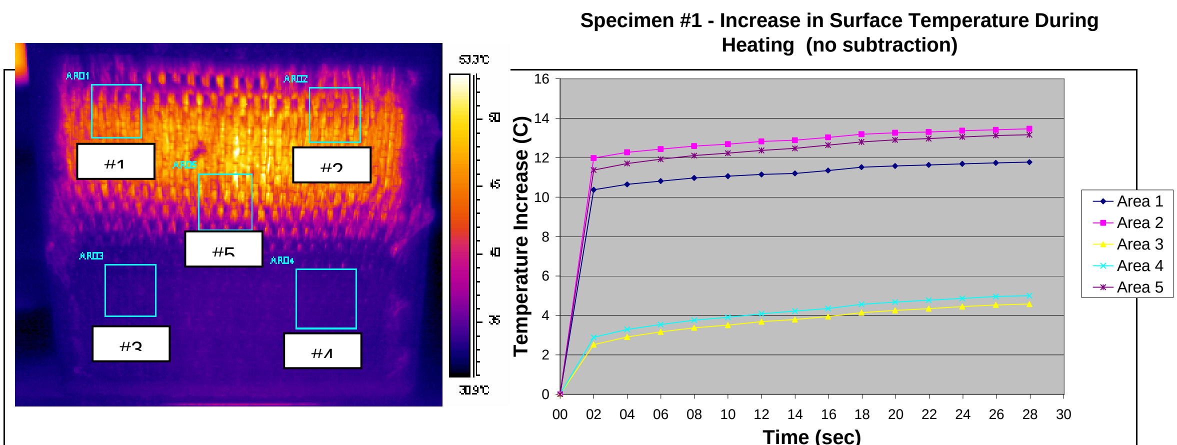

Figure 1. Specimen #1 – Heating with 500 Watt halogen lamp.

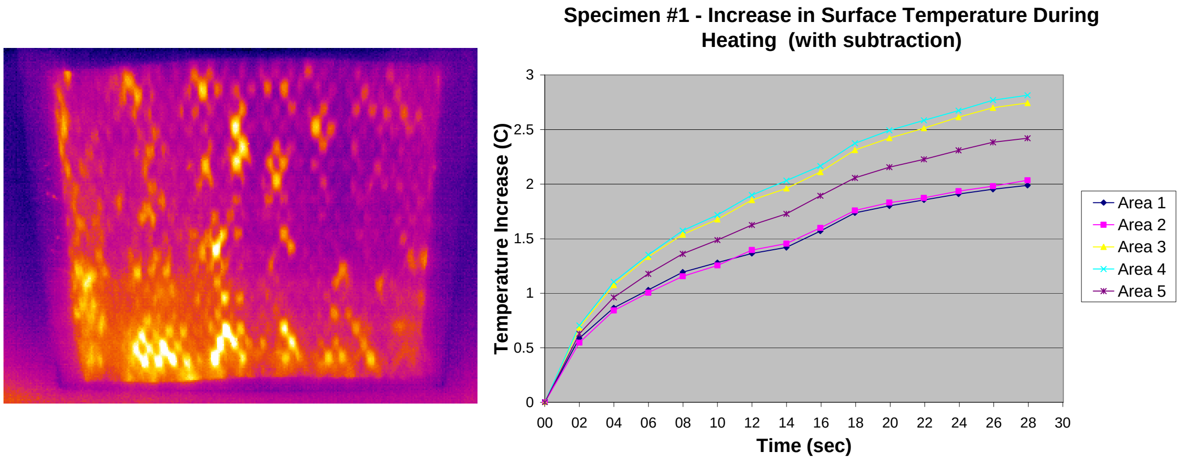

Figure 2. Specimen #1 – After 20 seconds heating with 500 Watt halogen lamp (reflections removed).

Figure 6. Specimen and test-setup for full-scale beam tests

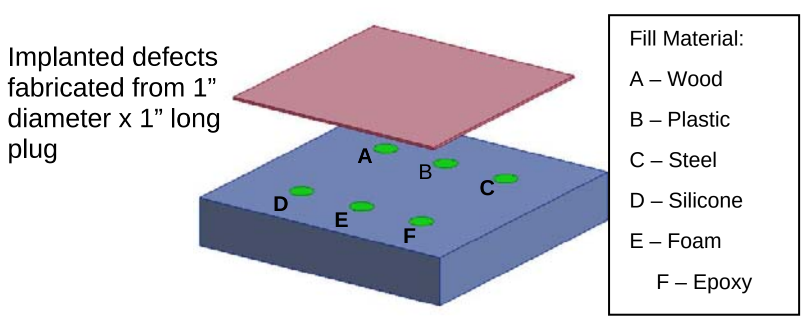

Figure 4. Specimen #3 – Implanted defects in concrete substrate

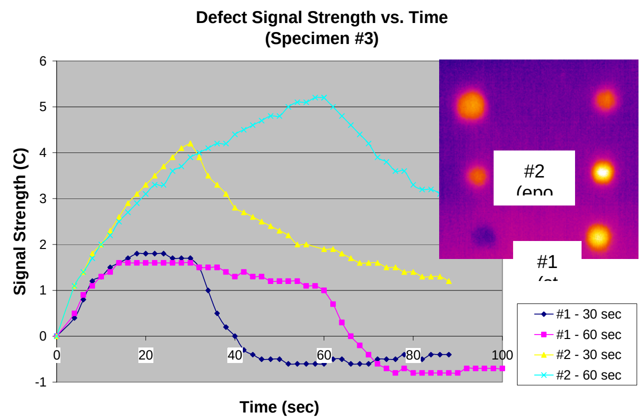

Figure 5. Specimen #3 – Defect signal strength vs. time

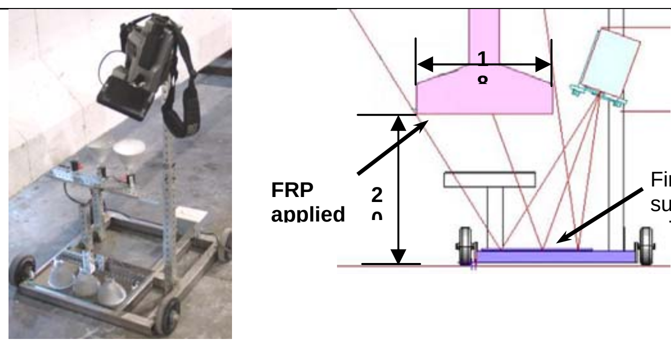

Figure 7. Schematic of scanner cart

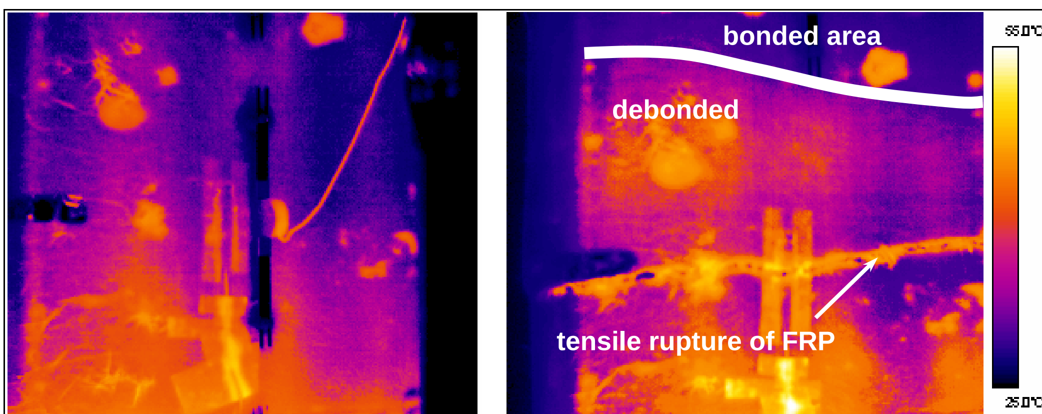

(a) midspan – before loading *(b) midspan – after failure*

Figure 8. Fiberglass spray-up system

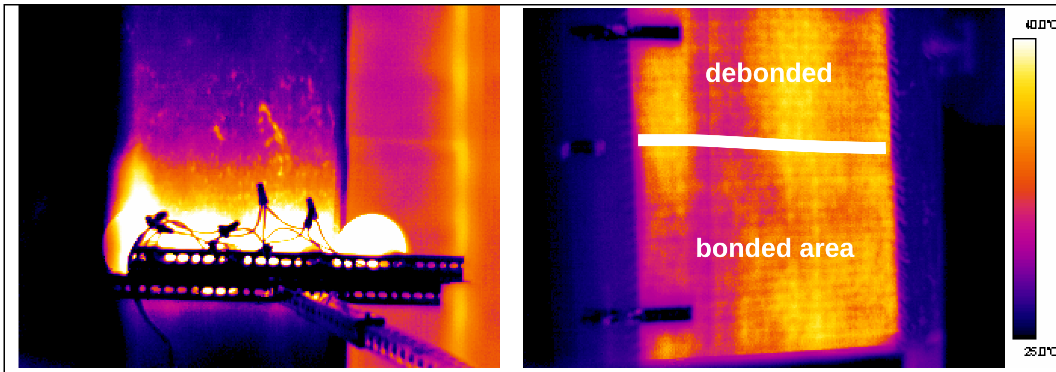

(a) Carbon-fiber – Epoxy System (during application) *(b) Carbon – Polyurethane System (after failure)*

Figure 9. Thermograms from Carbon - Epoxy and Carbon - Polyurethane systems

Girder#	**FRP System**	
	Fiber	**Matrix**
1	4-Layer Carbon	Epoxy
2	4-Layer Carbon	Water-Activated Polyurethane
3	Chopped Glass	Vinylester
4	3-Layer Carbon	Epoxy

Table 1: FRP Systems Used to Strengthen Full-Scale AASHTO Girder